BCSJ

Selected Paper

Comparison of Structure/Function Correlational Property of Three Kinds of Gemini-Type Thixotropic Surfactants Capable of Forming Crystalline Nanofiber Based on Hydrogen Bonding—Solid-State Structure, Two-Dimensional Molecular Film Forming, and Epitaxial Growth Behavior—

Manami Iizuka,[1] **Yuto Nakagawa,**[1] **Yuma Moriya,**[2] **Eiichi Satou,**[3] **and Atsuhiro Fujimori***[1]

[1]Graduate School of Science and Engineering, Saitama University,
255 Shimo-okubo, Sakura-ku, Saitama 338-8570, Japan

[2]Faculty of Engineering, Saitama University, 255 Shimo-okubo, Sakura-ku, Saitama 338-8570, Japan

[3]R & D Dept. Laboratory Additive Unit, Kusumoto Chemicals Ltd.,
4-18-6 Benten, Soka, Saitama 340-0004, Japan

E-mail: fujimori@fms.saitama-u.ac.jp

Received: December 11, 2017; Accepted: February 12, 2018; Web Released: April 24, 2018

Atsuhiro Fujimori
Dr. Atsuhiro Fujimori received his Ph.D. (2002) from Saitama University under the guidance of Prof. Hiroo Nakahara in the field of formation and structure of Langmuir-Blodgett films. After his experience as a post-doctoral researcher of JSPS, he became an assistant professor in Prof. Toru Masuko's Laboratory at Yamagata University in 2003 and widened her research to solid-state structure of crystalline polymers. He joined the department of graduate school of science and engineering, Saitama University, as an associate professor (2011).

Abstract

In this study, we compare and investigate both microscopic molecular packing and mesoscopic morphogenetic behavior in two-dimensional (2D) organized films/three-dimensional (3D) solids of three kinds of Gemini-type diamide surfactants that systematically differ in terms of their chemical structure. The gelation of the surrounding medium is promoted by growing crystalline nanofibers of these surfactants, and the disappearance of these nanofibers and solvent reflow are caused by the application of a force on the corresponding gel because these surfactant molecules are considered potential thixotropic agents. The layer structure and sub-cell in the 3D crystals of surfactants are formed by the association of van der Waals force and hydrogen bonding because the mechanism responsible for crystalline nanofiber formation is intermolecular hydrogen bonding. In the monolayer on the water surface, only surfactant molecules having a hydroxyl group in the hydrophobic chain formed crystalline nanofibers. The introduction of hydroxyl groups into the hydrophobic chains also promoted a single-phase molecular conformation in 3D crystals. However, the absence of hydroxyl groups in the hydrophobic chain promoted the growth of the nanofibers in the cast film, whereas the introduction of hydroxyl groups in the hydrocarbons improves the thixotropic property itself. In addition, the epitaxial growth of nanofibers upon the addition of a growth aid was promoted by the absence of hydroxyl groups.

Keywords: Gemini-type diamide surfactant | Crystalline nanofiber | Hydrogen bonding

1. Introduction

Thixotropy is defined as "a phenomenon in which fluidity temporarily increases when strain and stress are applied, viscosity decreases and returns to its original state when flow stops."[1,2] The thixotropy phenomenon is observed in foods such as mayonnaise and tomato ketchup, as well as waste-oil treatment agents, ballpoint pen inks, and bone marrow spinal fluid. On the contrary, dilatancy[3,4] is a phenomenon whereby solidification phenomenon occurs only when an external force is applied, whereas a flow is observed by standing still. In recent years, both thixotropy and dilatancy have tended to be recognized as macroscopic displacement phenomena, although attempts have been made to obtain control using a collaborative phenomenon from a molecular assembly level that transcends hierarchy.[5] When actively using this phenomenon in industrial fields such as paints, a fiber-growth technique is employed in solvents using additive molecules.[6] This fiber is a characteristic crystalline fiber derived from hydrogen bonding,[7] and the reflow of the solvent is caused by the decay of nanofiber growth and breaking hydrogen bonds (Figure S1). Hydrogen bonds that are generated during the regrowth of nanofibers are weaker compared to universal gel formation,[8,9] and they change cooperatively and hierarchically by external force induction.[10] Previously, 12-hydroxystearic acid[11,12] which is an ecological material obtained from castor oil, has been successfully utilized as a thixotropic agent, and has been commercialized.[13] However, the use of a low-molecular-weight compound having a low vapor pressure has limitations in terms of its application[14] as a dripping preventive agent or anti-settling agent for paints. However, molecules having hydrogen-bonding capabilities can improve thermal stability without the need for polymerization by increasing the number of hydrogen bonding sites.[15,16] Therefore, the three Gemini thixotropic molecules evaluated in this study are gemini-type[17,18] diamides having hydrocarbons. Actually, its performance has already been determined, and thixotropic agent molecules with the -OH group at the 12-position in a hydrophobic stearyl chain[6] are not inferior to other derivatives used in this study for all cases. Therefore, there is a possibility that the degree of microscopic hydrogen bonding will affect thixotropic physical properties. However, changes in the molecular level/functional group level cannot directly affect macroscopic viscoelasticity beyond the scale hierarchy.[19,20] On the medium scale, it appears that the molecular arrangement and packing, aggregation state, and morphology are hidden. In a previous study, we evaluated the structure and growth behavior of nanofiber in the cast film of diamide derivatives with two hydrocarbons obtained from castor oil,[6,21] a charge-transfer complex including tetrathiafulvalene (TTF),[22] and topological polymer.[23] In particular, it has been found that the addition of montmorillonite[24,25] particles subjected to organo-modification[26,27] at the surface induces remarkable fiber growth for Gemini-type diamide nanofibers having two hydrocarbons. However, the degree of growth of the nanofibers may not necessarily have a significant influence on the gelling of the contacting solvent. Hence, because we considered that it is important to explain the higher-order structure and its influence on the functionality caused by the difference in molecular structure, in this study, we compared the organization behavior of molecular species using the method involving interfacial molecular films.

By the way, diamide-based surfactants containing two hydrocarbons used in this study are materials that have already been put to practical use as “thixotropic additives” for automobile paints. The required function is to be able to apply a paint containing it and to prevent dripping after application. Since it is an amphiphilic chemical structure, it can be dispersed without phase separation both in the aqueous and in the oil systems and can be effectively used particularly for oil-based paints containing moisture such as paint.[28] In addition to the nanofiber formation in the medium by the formation of a hydrogen bonding network, the presence of the hydroxyl group is more easily dispersed in an aqueous system than a general-purpose surfactant, and the molecular design corresponds to chemical structure for which stability of the interface monolayer is relatively low. The difference from the gelator is that it includes the industrial requirement that “the solvent containing it can be applied to a paint”. On the other hand, these like hydrogen bonding networks tend to be broken and easily reproduced. Further, since the thermal stability of the compound itself is required, amide-based compounds are often formed by dehydration condensation.

In this study, we compare three Gemini-type diamide derivatives having two hydrocarbons obtained by condensation. There are 2:1 condensates of 12-hydroxystearic acid:hexamethylenediamine, stearic acid:hexamethylenediamine, and stearylamine:octanedioic acid. As an evaluation, the influence of the thermal behavior and solid-state structural formation exerted by intermolecular hydrogen bonds are investigated using thermal analysis, infrared (IR), and powder X-ray diffraction (XRD). Furthermore, the development of an organized molecular film was carried out at the air/water interface, and the fiberizing ability in the monolayer is evaluated from the viewpoint of the presence or absence of the hydroxyl group in the hydrophobic chain, and the crystallinity of the textured film was also examined. In addition, pseudo-thixotropic behavior was observed based on the state of spontaneous fiber growth in these cast films, and we compared the fiber-growth behavior when adding an effective growth aid to them (Figure 1). This study focuses on the comparison of the solid-state structure and the behavior/molecular arrangement in the organized films of three kinds of amphiphiles having the ability to impart thixotropic properties to the contacting solvent. Although this paper includes discussion of predicting the origin of thixotropy on the way, details will be discussed the next report. Discussions are being developed in this paper assuming that the high thixotropic performance and the degree of growth of nanofibers have almost equivalent implications.

2. Experimental

2.1 Synthesis and Characterization of Three Kinds of Amphiphilic Diamide Derivatives. Condensation reactions of 12-hydroxystearic acid:hexamethylenediamine, stearic acid:hexamethylenediamine, and stearylamine:octanedioic acid (2:1 mole ratio) were performed, respectively. During the synthesis, triphenyl phosphite and pyridines were used as the condensing agent and catalyst, respectively. The resulting compounds were identified *via* nuclear magnetic resonance (NMR), mass spectroscopy, and elemental analysis.[6] The obtained materials (Figure 2, *N*, *N*′-1,6-hexanediyl-bis-12-hydroxy-octadecanamide, *N*, *N*′-hexane-1,6-diyldistearamide, and *N*, *N*′-dioctadecyl octanediamide) were purified by recrystallization, and their purity was confirmed by performing thermal analysis. In order to estimate the sublimation or thermal-degradation behavior, we performed thermogravimetric (TG) analysis with an SII TG/DTA 3200 in N_2. Furthermore, the phase-transition behavior was estimated by differential scanning calorimetry (DSC, SII DSC6200). Figure S2 shows the gelation test of the monomers and synthetic samples at solvent introduction, and the drop experiment by visual observation. Although stearic acid had no gelling ability, 12-hydroxystearic acid, its condensate, and diamide derivative of stearic acid showed gelling ability in the solvent.

2.2 Characterization of Three-Dimensional Structures in Bulk and Their Spin-Cast Films. The spin-cast films of three kinds of Gemini-type diamide derivatives with two hydrocarbons and a mixture with organo-modified layered silicate

© 2018 The Chemical Society of Japan

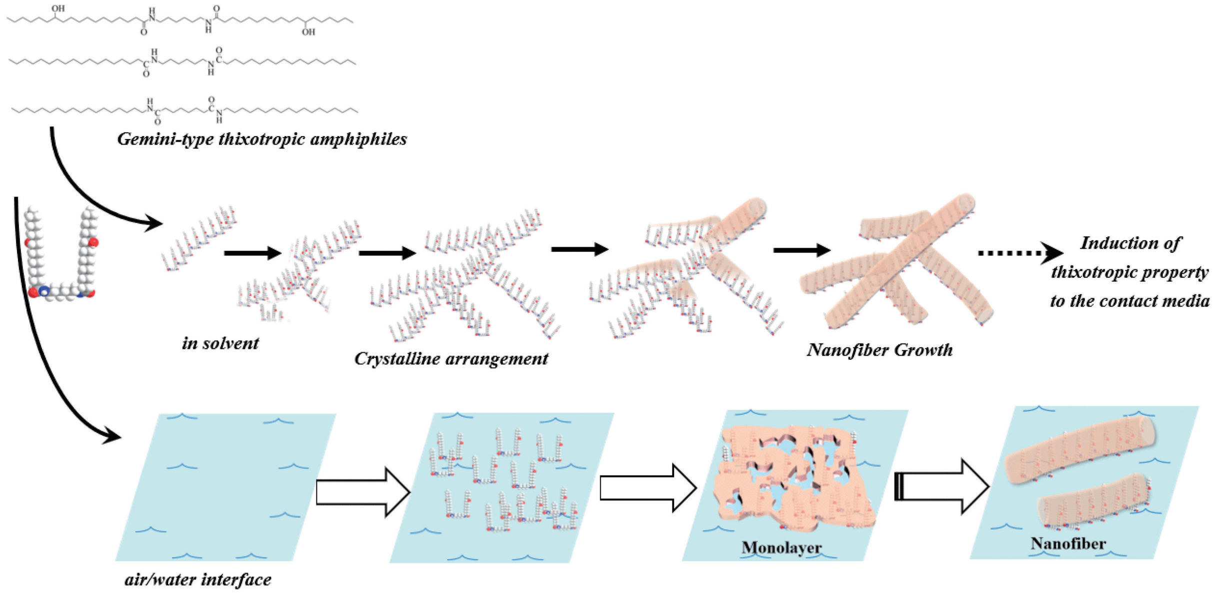

Figure 1. Research strategy of this study.

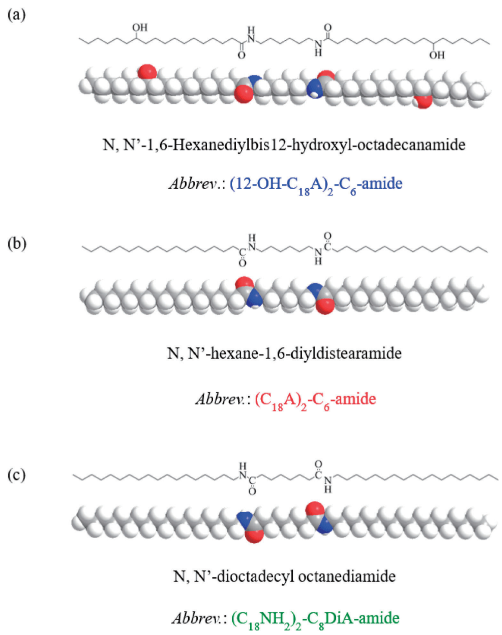

Figure 2. Chemical structure and 3D models of three kinds of Gemini-type amphiphiles used in this study.

were formed from a xylene:ethanol (9:1, v/v) mixed solution at 100 °C. From the evaluation of solution temperature dependency at spin-casting, uniform morphology was always obtained without dependence at over 100 °C. Organo-modified montmorillonite (MMT) was prepared using a surface-modification method from natural MMT (Figure S3(a)) and long-chain quaternary ammonium cations (Figure S3(b)) at an oil/water interface.[26] Powder XRD measurements of both the bulk and cast film samples were obtained using an X-ray diffractometer (Rigaku, Rint-Ultima III, Cu-Kα radiation, 40 kV, 30 mA) equipped with a graphite monochromator. IR spectra of the samples were obtained using an IR spectrometer (Bruker AXS TENSOR II). Further, small-angle X-ray scattering (SAXS) was used to estimate the long periods of the layer structure. The apparatus (Nano-Viewer, Rigaku Co. Ltd.) was operated at 40 kV and 30 mA to generate CuKα radiation (λ = 0.1542 nm).

2.3 Monolayer Formation for Three Kinds of Gemini-Type Diamide Derivatives with Two Hydrocarbons at the Air/Water Interface. Monolayers of the Gemini-type diamide derivates ($\sim 1.0 \times 10^{-4}$ M) were formed by spreading from a $CHCl_3$ solution comprising a small amount of trifluoroacetic acid (TFA), on the surface of distilled water (resistivity: approximately 18.2 MΩ•cm). After evaporation of the $CHCl_3$ for 5 min, π–A isotherms were recorded at a compression speed of 4.8 $cm^2 \cdot min^{-1}$. The air/water interface was kept at a constant temperature of 12 °C by the circulation of temperature-controlled water around the trough. Measurements of the monolayer properties and Langmuir-Blodgett (LB) film transfer were obtained using a USI-3-22 Teflon-coated LB trough (USI Instruments).

2.4 Study of Surface Morphology and Estimation of Molecular Arrangement. The surface morphologies of the transferred monolayers were observed using a scanning probe microscope (atomic force microscope (AFM), SII Nanotechnology, SPA300 with an SPI-3800 probe station) and microfabricated rectangular Si cantilevers with integrated pyramidal tips, by applying a constant force of 1.4 $N \cdot m^{-1}$. In this study, AFM observations were performed in the tapping mode (dynamic force mode). XRD samples were then transferred onto a glass substrate using the LB method (20 layers, a subphase temperature of 15 °C, and a surface pressure of 35 $mN \cdot m^{-1}$). The large spacing between the layers in the films was measured using an out-of-plane X-ray diffractometer (Rigaku, Rint-Ultima III, Cu-Kα radiation, 40 kV, 30 mA) equipped with a graphite monochromator. We determined the in-plane spacing of the two-dimensional (2D) lattice of the films using an X-ray diffractometer with different geometrical arrangements[29,30] (Bruker AXS, MXP-BX, Cu-Kα radiation, 40 kV, 40 mA, a customized instrument), and it was equipped with a parabolic graded multilayer mirror. The X-rays had an incident angle of 0.2°, and the films were scanned at a speed of 0.05°/20 s, as a result of which the in-plane XRD measurements had monomolecular resolution.

In the case of AFM observation, mica substrate was used for both single layer LB film and cast film. When the surface of the glass substrate was observed by AFM, it was judged that this substrate was inappropriate for morphological observation because it was very rough. However, since information can be averaged by XRD analysis, it was deposited on a glass substrate comparing the periodic structure of the LB multilayers. In the case of LB films, it is thought that the factors that mainly form the structure are large due to the intermolecular interaction in the lateral direction. I thought that the influence from the surface roughness of substrate would be less if multilayered. As mention above, considering the probing area, we avoided the use of glass substrates for morphological observation, and we used glass substrates for XRD analysis of layer period and in-plane spacing.

The experimental conditions used in this study are based on the conditions recognized as well-defined in a report of K. Blodgett in 1935 and the interfacial molecular film study.[31] It has assumed time, temperature, humidity, compound purity, substrate type, and film formation conditions as prescribed by Langmuir et al.,[32,33] in order to compare with previously reported data.

3. Results and Discussion

3.1 Thermal Behavior and Molecular Packing of Three Kinds of Diamide Derivatives in Bulk. First, in order to estimate the influence of the hydroxyl group at the 12-position in the hydrophobic chain, we investigated the thermal behavior and molecular arrangements of the three kinds of Gemini-type amphiphiles in bulk. Figure 3(a) shows the thermogravimetric (TG) curves of these three compounds. Under nitrogen atmosphere, all of the thermal degradation temperatures of these compounds are 300 °C, which is very high for the degradation temperature of a general low-molecular compound. In particular, the thermal degradation temperature of a Gemini-type molecule having a hydroxyl group at the 12-position in the hydrophobic chain is very high. In this regard, when the TG measurement of this compound is done in the atmosphere, a residue is generated, and the value of the weight loss does not reach zero. In other words, because of the influence of intermolecular hydrogen bonding, these amide-based compounds exhibit behavior closer to the thermal degradation behavior of general polymers than those of the sublimation phenomenon of low-molecular-weight compounds. In particular, the existence of a hydroxyl group at the 12-position increases the hydrogen bonding site, and it is expected that the thermal degradation temperature would be enhanced with the development of the hydrogen bond network.

Figure 3(b) shows the DSC curves of these three kinds of compounds. All of the compounds melt within the range of 135–160 °C, and the figure shows the crystallization behavior within the range of 125–145 °C. Although no systematic differences have been observed based on the chemical structure, all three of the compounds were crystalline compounds.

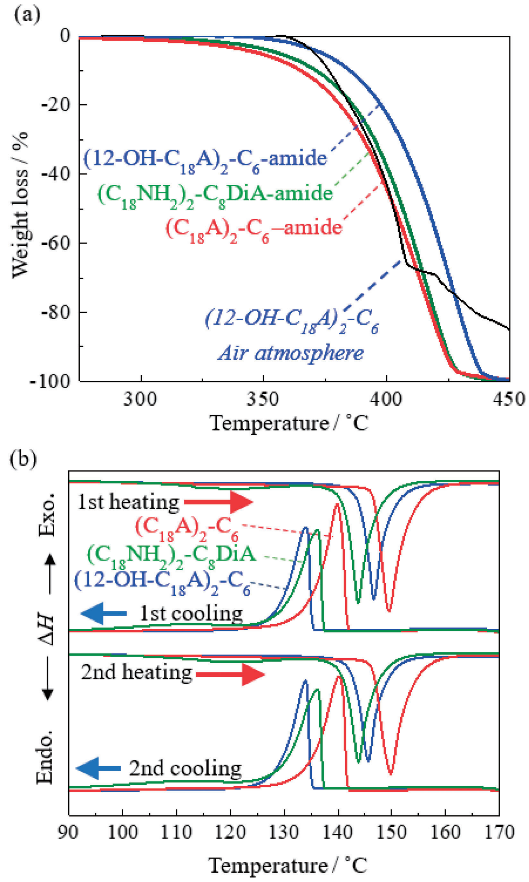

Figure 3. (a) TG curves of diamide derivatives having two hydrocarbons used in this study under the N_2 purge and in air atmosphere. (b) DSC thermogram of purified diamide derivatives having two hydrocarbons (scanning rate; 10 °C min^{-1}).

Figure 4(a) shows the powder XRD profile of these three kinds of Gemini-type amphiphiles. The peaks that were developed based on the long period of the *c*-axis length are confirmed in the low-angle region of the profiles of all compounds. The fourth- or fifth-order reflections are confirmed, suggesting the formation of a highly ordered layer structure. From the comparison with the results obtained during the small-angle X-ray scattering measurement described later, the values of the primary periodic length are 48.5, 42.5, and 44.2 Å at this point. Figure 4(b) shows the IR spectrum in the bulk of these three kinds of compounds. Although the spectra of all of the compounds clearly indicate the amide bands (1500–1600 cm^{-1}), the bands on the high wavenumber side are also important (Figure 4 (c)). It can be seen that both the O-H stretching vibration and the N-H stretching vibration band, which exist in the vicinity of 3700 cm^{-1}, are shifted to 3200 to 3300 cm^{-1}. Examining previous literature[34,35] and IR data books, it seems likely that as a result of strong intermolecular hydrogen bonding, free O-H and N-H stretching vibrations greatly cause a low wavenumber shift. Although the degree of the shift is small in the case of dimerization, it is known that the degree of shift is large in the case of homogeneous multimer. In particular, the molecule with the -OH group shows corresponding bands around 3200 cm^{-1}, and it can be easily attributed. These results indicate that all of the N-H groups in the amide group and the -OH group in the hydrophobic chain are involved in intermolecular hydrogen bonding.

© 2018 The Chemical Society of Japan

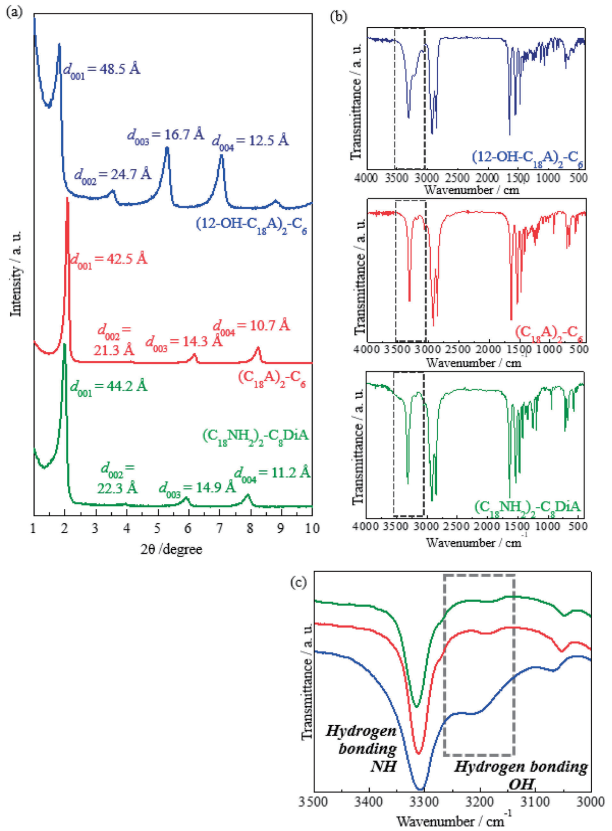

Figure 4. (a) Powder X-ray diffraction profile of diamide derivatives having two hydrocarbons in bulk. (b) IR spectra of diamide derivatives having two hydrocarbons in bulk. (c) Enlarged IR spectra of region of hydrogen bonding O-H and N-H bands.

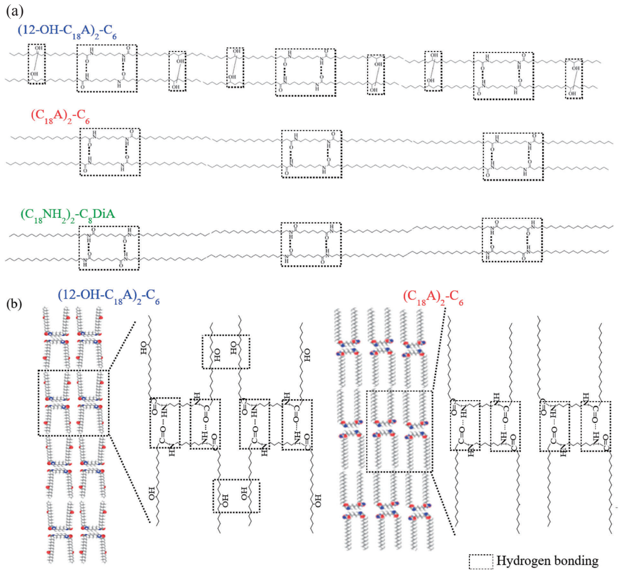

Figure 5. Schematic illustration of two kinds of potential molecular arrangements of diamide derivatives having two hydrocarbons in bulk. (a) Extended chain model. (b) Double-layered structure model.

Here, we predict the molecular arrangement in the solid phase, taking into consideration the formation of intermolecular hydrogen bonds. Two conformations can be considered simply. One is the formation of extended chain crystals (ECCs). Figure 5(a) shows an example of an ECC conformation for three kinds of compounds. Amide groups and hydroxyl groups individually interact with each other, and molecules arrange and pack with the same phase, so that a highly ordered layer structure is formed. In the compounds having no hydroxyl group, the only interaction between the hydrophobic chains is the van der Waals force. In this case, the extended molecular length is much greater than 50 Å for each molecule. In other words, based on the value of the XRD first-order period, a molecular arrangement having a relatively large tilted angle is predicted.

However, the molecular arrangement shown in Figure 5(b) is also a potentially good candidate as inference. At first glance, it seems that the model where there is a space between the alkyl chains is irrational. However, in fact, the corresponding space does not exist. This case indicates model in which two alkyl chains are densely packed. In this model, the hexamethylenediamine linker is random and does not stretch. This evidence is supported from the emergence of multiple diffraction peaks showing hydrocarbons densely packed in the lateral direction in the vicinity of d = 4 Å in the powder XRD shown for the following Figure S5. In addition, there are many reports of a stabilized double layered structure of such surfactant molecules, and support inference.[6] In this case, the bimolecular period corresponds to the first-order periodic value. It is generally well known that many surfactant molecules form such a double-layer structure.[36] Because the molecular length of stearic acid is about 25 Å, there is good agreement between the molecular length and the long-period value. Hydrogen bonds occur between amide groups along the *c*-axis at interlayers, and they occur between alkyl chains along the transverse direction between hydroxyl groups. At first glance, these results appear reasonable in Figure 5(b), but they are not well confirmed. Therefore, this approach is considered together with the result of the subsequent small-angle X-ray scattering measurement.

Figure 6(a) shows the small-angle X-ray scattering patterns and profiles of the three compounds used in this study. Because all of the SAXS patterns are annular, it finds that these measurements are performed for molecules in an isotropic state. Interestingly, the compound with hydroxyl groups indicates only a single period, while the other two compounds show two long-period values. A long period spacing 50 Å could not be confirmed because of the detection limit in WAXD. Compared with the results of powder X-ray diffraction, it can be considered that the values of the XRD first period and the SAXS period of the hydroxyl group-containing compound are the same at the error level. However, in the other two compounds, short-value periods on the high q value side correspond to the XRD first-order periods, and the first-order periods exceeding 50 Å in both cases are also shown. From the XRD results, we observe that scattering peaks on the high q-value side are based on a developed layer structure showing XRD high-order reflection. On the contrary, from the high intensity of these SAXS peaks, it is believed that these values of the period reflect lengths with a large electron-density difference. Based on the above, we estimated the model diagram shown in Figure 6(b).

© 2018 The Chemical Society of Japan

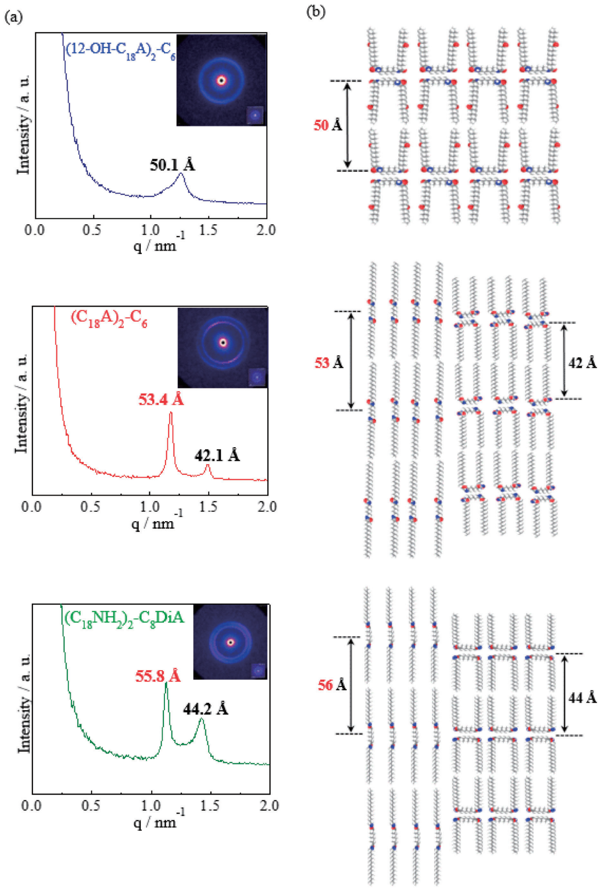

Figure 6. (a) Small-angle X-ray scattering patterns and profiles of three kinds of Gemini-type diamide derivatives having two hydrocarbons in bulk. (b) Expected phase models of three kinds of Gemini-type diamide derivatives.

It is clear that the derivative of 12-hydroxystearic acid has a double-layered single-phase structure. However, derivatives of stearic acid and derivatives of stearyl amine are expected to be mixed crystals. In this case, it is reasonable to assume that a developed multilayer structure and elongated chain crystals are mixed. Judging from the height of the vertical-axis intensity of SAXS, it is expected that there would be repeated periods between the high-density packed state of long alkyl chains and the low-density aggregated state of linker moiety. In the formation of a double-layer structure, it is considered that the linker part, which is randomized owing to strong interactions between long chain alkyls, is elongated in the extended chain crystal to form a low-density phase. In other words, it is considered that the hydroxyl group at the 12-position has the effect of forming a "monophasic" molecular group. This is an effect of intermolecular hydrogen bonding, which occurs between hydroxyl groups.

Based on the above-mentioned results, it was aimed to acquire related information by measuring temperature control IR (Figure S4) and temperature control XRD (Figure S5). Almost no change was confirmed in the temperature-controlled IR measurement.

However, the temperature-controlled WAXD also showed changes other than the octadecylamine derivative which the solid-solid phase transition was confirmed in DSC thermograms. In the 12-hydroxystearic acid derivative, a shift in the layer period (Long Spacing) by heating was not confirmed. A change was observed in the diffraction peaks near $2\Theta = 20^\circ$ ($d = 4$ Å) called Short Spacing. However, this seemed to be a peak shift corresponding to the change in lattice size by heating. On the other hand, as the stearic acid and the stearylamine derivatives heated, the long spacing peaks shifted by a small angle side and the interlayer spacing broadened. Also, in each case, a change in the short spacing appeared. This is probably because the mixed crystal of extended chain crystal and double layered crystals is formed, and the structure is likely to transfer due to molecular motion by heating. Although the driving force of structural formation is an enhanced van der Waals interaction between alkyl chains in any case, it seems that mixing of different layer structures is likely to lead to disorder of arrangement.

3.2 Monolayer Morphology and Molecular Arrangement of Three Kinds of Diamide Derivative with Two Hydrocarbons in Two-Dimensional Films. Up to the present, the solid-state structure of three kinds of Gemini-type amphiphiles capable of imparting thixotropic properties to the contact solvent have been compared. The reversal of the amide bond and the length of the linker length do not significantly affect the structure formation. The presence of the hydroxyl group at the 12-position in the hydrophobic chain has a significant effect, which is more owing to the influence of intermolecular hydrogen bonds that arise from this –OH group rather than the presence of the hydroxyl group itself. In fact, the thixotropy imparting property is also remarkable in the derivative of the 12-hydroxystearic acid. Subsequently, the state of comparing these three compounds is at the air/water interface and in a complete-layer structural organization. The thixotropy imparting property is aimed to be expressed even at extremely thin thickness as a monolayer. Because the induction of the thixotropic ability by additives is accompanied by fiber growth, for introduction into painting media, it is desired to suppress fiber growth in the thickness direction. In order to prevent the nonuniformity of the coating film owing to contamination and light scattering, fiberization in a monomolecular film state is required. The aim is to determine whether it is possible to form a monolayer fiber, and to clarify the correlation between the monolayer fiberization and chemical structure.

Figure 7(a) shows the behavior of the monolayer on the water surface for the three kinds of Gemini-type surfactant molecules used in this study. As shown in previous studies,[6] the surface pressure-area isotherm of compounds with hydroxyl groups shows clear 2D phase transitions. Though the π-A isotherm of $(12\text{-OH-C}_{18}\text{A})_2\text{-C}_6$-amide is very complicated, this result is reproducible as long as it is the same temperature condition of subphase. Also, since the presence of impurities is not confirmed in the results of NMR and thermal analysis, this material is considered to be a pure material. It seems that the cause of the tortuous π-A curve of this compound is the promotion of intermolecular hydrogen bonding between the hydroxyl groups present in the hydrophobic chain. As the surface pressure rises, formation of intermolecular hydrogen bonds becomes noticeable as the intermolecular distance approaches. The morphological changes at this time, and the change of the

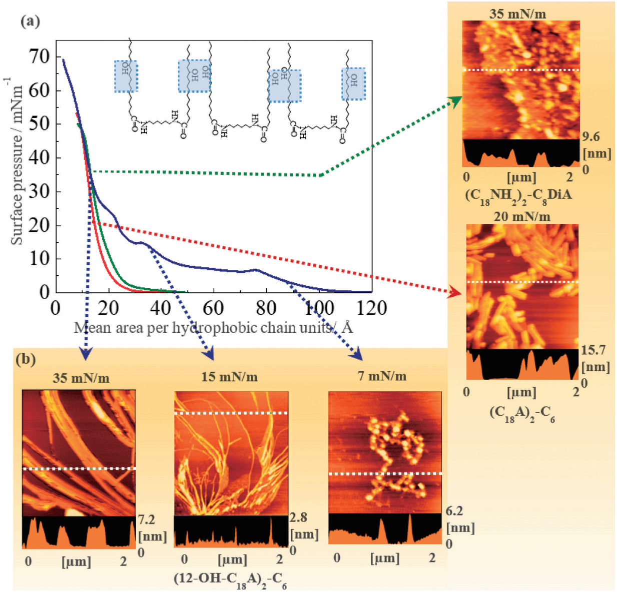

Figure 7. (a) Surface pressure–area isotherms of monolayer on the water surface of diamide derivatives having two hydrocarbons transferred at several surface pressures at 12 °C. (b) AFM images of monolayer on solid substrate of diamide derivatives.

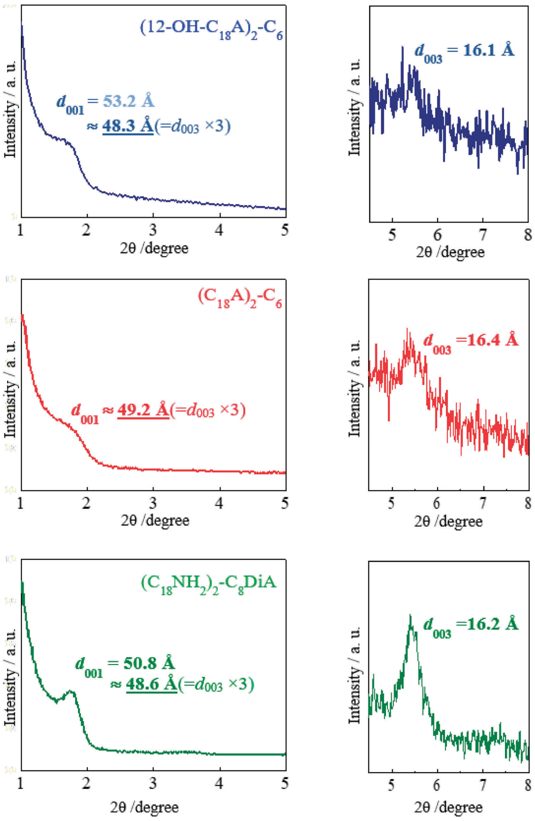

Figure 8. Out-of-plane XRD profiles of LB multilayers of diamide derivatives having two hydrocarbons transferred at 20 or 35 mN m^{-1} and 12 °C.

isotherms due to the temperature dependence of subphase has been shown in the previous report.[6,30,33] It is expected that the transition will be linked to the promotion of hydrogen bonding because the dot-like domains become fibrillated and grow while repeating the transition (corresponding AFM images of Figure 7(b)). Interestingly, if the hydroxyl group at the 12-position is lost, the phase-transition behavior cannot be seen on the π-A curve. In this case, since it is confirmed that the AFM image of the transferred monolayers on the solid indicates sheet-like texture and aggregated crystallite film, these are observed that the monolayer fiber cannot be formed. As shown in the illustration in Figure 7(a), because the amide bond site is present under the water surface and cannot participate in intermolecular hydrogen bonding, it is expected that only compounds with a hydrogen bonding site in the hydrophobic chain can be made into fibers.

It should be noted that the interfacial conformation of these molecules is considered to equally place two amide sites under the water surface as a hydrophilic group. Considering amphiphilicity, it is difficult to consider other possibilities. The height information of the AFM in the low surface pressure region almost corresponds to this prediction. However, the corresponding height information in high surface pressure region has not been accurately grasped from AFM observation. The height information of the AFM as shown in Figure 7(b) is the highest numerical value in the 2 × 2 µm^2 probing area. Actually, as a locally averaged height, it can reach a value about 3 nm. However, especially in the high-pressure region of transferred surface pressure, the grown single-layered fibers and the crystallites themselves partially overlap, and the height information is estimated to be large. Further examination and experimentation may be necessary for this part. It may be regarded as a feature of fiber/microcrystal growing together with increasing surface pressure. In this case, if multilayers are formed by the LB method, the formation of a double-layer structure, which is inevitably predicted in the bulk state, can be achieved. Figure 8 shows the out-of-plane XRD results for these three kinds of compounds with respect to the 20 LB layers. All of the multilayers exhibited a high degree of layered regularity showing a third-order reflection. Here, because the d-spacing value calculated from the high-order reflection is more accurate than the peak position on the low-angle side, we calculated the first-order period. The d_{001} period obtained here is a distance not exceeding 50 Å, which confirms that the estimation of the double-layer structure period (estimated from the powder XRD) in the bulk state was appropriate. Furthermore, from the results of the in-plane XRD for these samples, crystalline peaks were all confirmed, and we determined that all of the multilayers were crystalline films (Figure 9(a)). In this case, since LB film of hydroxyl group-containing molecules corresponds to multilayers of "a single-layer fiber film", it is found that this compound can form a crystalline monolayer fiber. This result shows the potential for the development of monolayer thixotropy because nanofibers that exhibit thixotropic properties are recognized as fibers having crystalline regularity in either case. Incidentally, as shown in the enlarged views of Figures 9(b) and 9(c), all of the O-H groups and N-H groups also form hydrogen bonds in the multilayers as a result of the IR. During the formation of a monolayer on a water surface, the amide group is present under the water surface

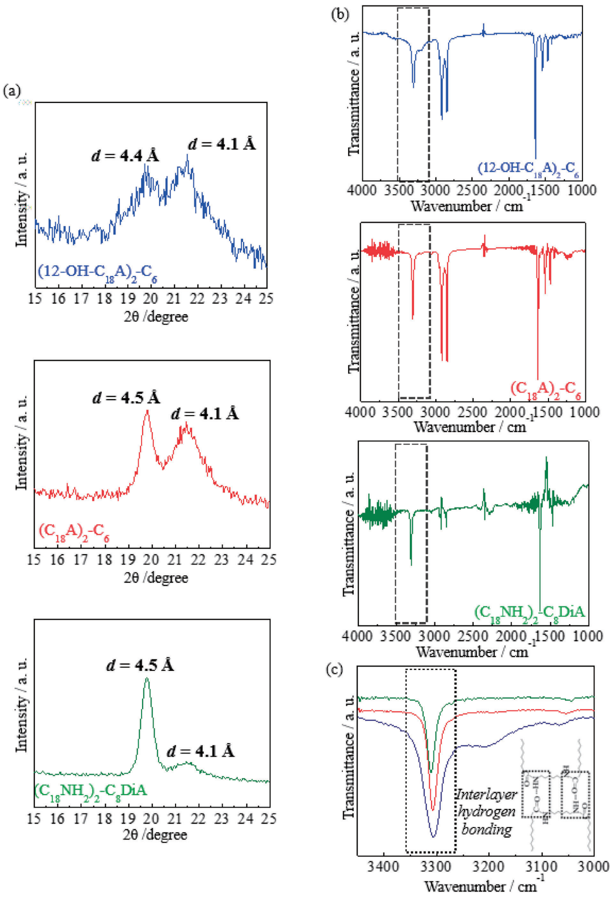

Figure 9. (a) In-plane XRD profiles and (b) IR spectra of LB multilayers of diamide derivatives having two hydrocarbons transferred at 20 or 35 mN m^{-1} and 12 °C. (c) Enlarged IR spectra of region of hydrogen bonding O-H and N-H bands.

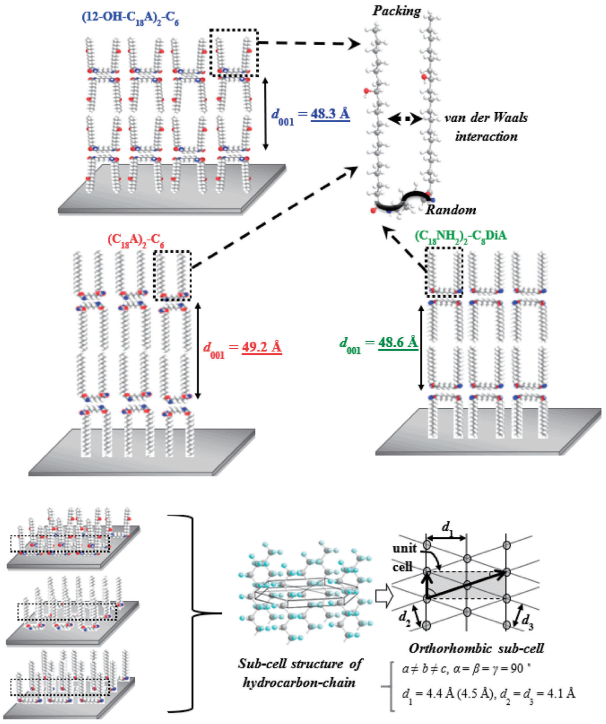

Figure 10. Schematic models of layer structure and sub-cell of hydrocarbons in LB multilayers of diamide derivatives having two hydrocarbons.

and cannot contribute to intermolecular hydrogen bonding. However, in the LB multilayers, it can form an interlayer hydrogen bond with hydrophilic groups that face each other, so all of the N-H groups are presumed to be involved in hydrogen bonding.

Figure 10 shows a model diagram of the molecular arrangement in LB multilayers based on the above discussion. All of the molecules form a developed layer structure in the LB film, and its first-order periodic value is less than 50 Å. All of the packing modes of molecular chains in the 2D plane are 2D orthorhombic systems,[37] and the in-plane periodic value is estimated to be 4.4 (or 4.5) Å and 4.1 Å.

3.3 Nanofiber Formation in Cast Films and Their Epitaxial Growth Behavior by Additive Growth Aid. In this section, we discuss the formation behavior of fiber morphology in the bulk state based on the above investigation. Three kinds of Gemini-type amphiphiles used in this study are thixotropic additive candidates. These additive molecules have the ability to form crystalline nanofibers derived from intermolecular hydrogen bonds in a solvent. Fiber growth in a solvent corresponds to a driving force for the development of thixotropy. Therefore, as an evaluation of a pseudo fiber growth in solvent, we carried out an AFM observation on a spin cast film (Figure 11(a)). As mentioned above, the function as a thixotropic additive of hydroxyl group-containing surfactant molecules is excellent. In addition, the origin of thixotropy is recognized as fiber growth in the medium. However, at first glance, the degree of fiber formation appears to be more prominent in the group of compounds having no hydroxyl group. Although relatively fine nanofibers are formed in the hydroxyl group-containing compound, the growth of the developed fiber, which leads to microfibers, is confirmed in the other two compounds. In the preceding study,[6] owing to the addition of organo-modified clay (montmorillonite) having a crystalline-layer arrangement as well as these fiber-forming compounds, the development of fibers by epitaxial growth was found from the similarity of layer spacing. When 1 wt% of organo-modified montmorillonite was added to all three compounds using this technique, the growth of mesoscopic fiber morphology was confirmed in all the compounds. Incidentally, as shown in Figure S6, there is a clear dependence on the concentration of organo-clay that is to be added as a growth aid. When 0.5 wt% was added, it is not easily distinguished from neat materials. In the case of the 5-wt% addition, because the growth progresses to such a degree that no significant difference can be confirmed for each compound, an additional 1 wt% was adopted in this study. Even under the same condition, there is a high degree of promotion of fiber growth of hydroxyl group-free compounds (Figure 11(b)). Since it is presumed that it may be due to the presence of hydrogen bonding network along a horizontal direction derived from hydroxyl groups in hydrophobic chain, it is assumed that there will be suppressed growth along the c-axis direction from the surface of organo-clay which is a layer structural material like a thixotropic agent

© 2018 The Chemical Society of Japan

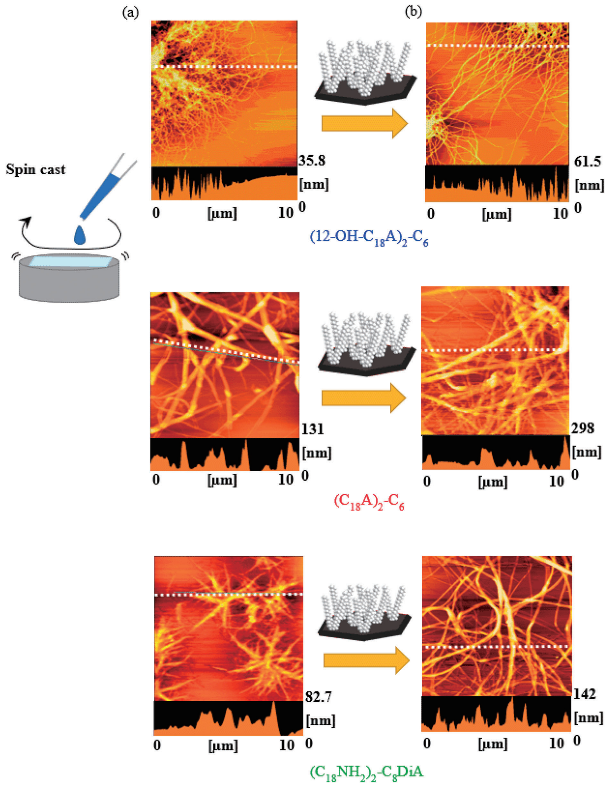

Figure 11. AFM images of spin-cast films of (a) neat diamide derivatives having two hydrocarbons and (b) their composite with 1 wt% organo-modified MMT, fabricated at room temperature.

molecule. However, it is also confirmed that the formation and growth of such fine nanofibers can impart more pronounced thixotropy to the contact medium. The relationship between the presence of the microscopic hydroxyl group and the hydrogen-bonding network formation, the growth style of mesoscopic nanofibers, and macroscopic thixotropic properties remains unclear. This is regarded as a molecular cooperative effect that transcends the hierarchy of materials. Current studies aim to determine whether the hydroxyl group at the 12-position is bonded to the asymmetric carbon. Preliminary experiments have confirmed the dextrorotatory behavior by circular dichroism spectra, as well as the right-handed spiral fiber growth of the molecules. Now, the explanation of the correlation between molecular chirality and morphological growth[38] is interesting, and it is positioned as a future study topic. In this point, rather growth entangled fibers estimated by a scanning electron and transmission electron microscopy (SEM and TEM) have already been observed (Figure S7). It was thought the origins of thixotropy in a bundled fiber form developed in an organization like observed by electron microscopy, not a thin elongated fiber as observed with AFM in the above data. Here, the measurement result of circular dichroism (CD) spectrum was also indicated (Figure S8(a)). As shown in Figure 8(b), no cotton effect is observed in all Gemini-type diamide derivatives and 12-hydroxy stearic acid in solution. However, in the cast film, the positive cotton effect was clearly observed only in the surfactant having 12-hydroxy stearyl chains with the highest thixotropic ability. On the other hand, the other two diamide-based surfactants that are inferior to other thixotropic properties, did not indicate the cotton effect in the CD spectra. In this case, these diamide derivatives formed only linear fibers in SEM images. That is to say, in compounds having excellent thixotropy, chirality due to mesoscopic structure formation is developed, and this is expected to be related to the origin of enhancement of this physical property. The contents of this research will be clearly indicated by research reports in the near future.

The presence of the hydroxyl group at the 12-position in the hydrophobic chain of the Gemini-type surfactant molecule affects the distinct structure formation and morphological growth. The monophasic formation of a layered structure and thin nanofiber growth, and the formation of single-layer nanofibers are realized by intermolecular hydrogen bonds that are derived from hydroxyl groups. The absence of a hydroxyl group leads to the microfiber formation of mixed crystals and a 2D microcrystalline monolayer, indicating that the presence or absence of one functional group clearly influences hierarchically the molecular arrangement and mesoscopic morphological formation. In this research, although it conducted a multilateral analysis, there are various methods for analyzing molecular packing and hydrogen bonding, and there is a possibility that new information can be obtained from these results. For example, since the result of ^{1}H NMR in solution, solid, or gel may be useful to understand the molecular packing among surfactants, Figure S9 showed ^{1}H NMR spectra of Gemini-type diamides used in this study under heating. It is presumed that this data makes it possible to pursue new facts by proactively analyzing though the resolution is not sufficient because of poor solubility of the sample.

4. Conclusion

In this study, we compared the molecular arrangement/packing on a microscopic scale and the morphological formation at a mesoscopic scale in 2D and 3D structures of three kinds of Gemini-type diamide amphiphiles that are systematically modified in the chemical structure (Figure 12). The amphiphiles used in this study are potential additives that induce thixotropic properties to the contact media. The origin of the expression of thixotropic properties is that additive molecules form crystalline nanofiber morphology in the medium by intermolecular hydrogen bonding. All three kinds of amphiphile used in this work are diamide derivatives with two hydrocarbons. The amphiphile having the highest thixotropy-imparting ability has a hydroxyl group at the 12-position of the two hydrophobic chains. Although all three kinds of thixotropic molecules are crystalline molecules forming highly ordered layer structures, the presence of the hydroxyl group at the 12-position improves the thermal degradation temperature, becoming a monophasic layer structure, and forms single-layer nanofibers at the air/water interface. The growth of fiber morphology was confirmed in the cast-film formation of each compound. The lack of hydroxyl groups in the long-alkyl chain promoted the growth of the nanofibers in the cast film, whereas the introduction of hydroxyl groups in the stearyl chains improves the thixotropic property to the contact media. Further, the epitaxial growth of nanofibers upon the addition of organo-modified clay was promoted by the absence of hydroxyl

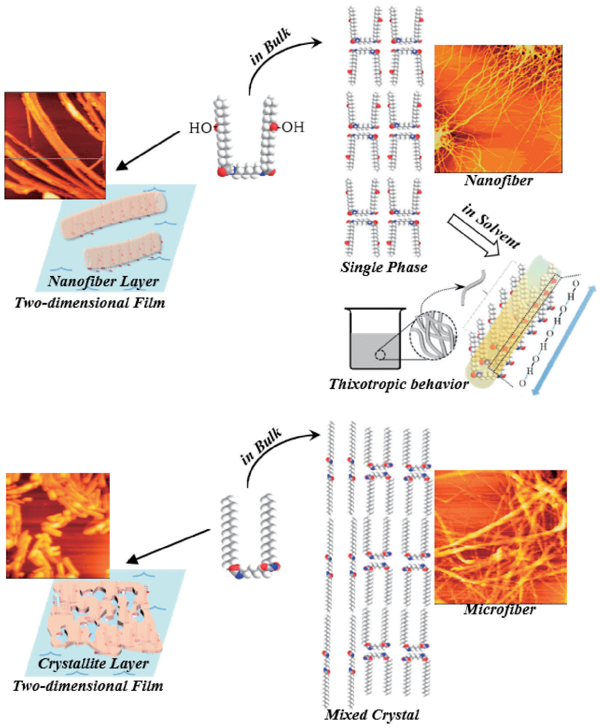

Figure 12. Schematic illustration of summary in this study.

groups. Attempts to compare the molecular arrangement/packing and morphogenesis of molecular groups that systematically differ in terms of the chemical structure under specific properties can be realized by understanding both the hierarchy of materials and the cooperation of molecules. It is essential to approach such a study from a multifaceted perspective by fusing multiple measurement/analysis technologies. From the results, it can be understood that there is actually a similarity in the structural formation/morphogenetic behavior of the molecular group, and we believe that these fundamental findings will help to develop practical materials.

The authors appreciate the support by the Ministry of Education, Culture, Sports, Science, and Technology (MEXT) for funding provided by a Grant-in-Aid for Scientific Research (C, 17K05986 (A.F.)). The authors thank Prof. Yuji Shibasaki, Iwate University for measurement of temperature-controlled NMR spectra. Further, authors would like to express our gratitude to Prof. Toru Mizuki at Toyo University for CD spectra and SEM observation.

Supporting Information

This material is available free of charge *via* the Internet at http://dx.doi.org/10.1246/bcsj.20170406.

References

1 J. Mewis, N. J. Wangner, *Adv. Colloid Interface Sci.* **2009**, *147–148*, 214.

2 H. Hoshizawa, Y. Minemura, K. Yoshizawa, M. Suzuki, K. Hanabusa, *Langmuir* **2013**, *29*, 14666.

3 M. D. Bolton, *Géotechnique* **1986**, *36*, 65.

4 H. A. Barnes, *J. Rheol. (Melville, NY, U. S.)* **1989**, *33*, 329.

5 S. E. Paramonov, H.-W. Jun, J. D. Hartgerink, *J. Am. Chem. Soc.* **2006**, *128*, 7291.

6 M. Iizuka, Y. Nakagawa, K. Ohmura, E. Satou, A. Fujimori, *J. Colloid Interface Sci.* **2017**, *498*, 64.

7 Z. Liu, G. Liu, Y. Wu, D. Cao, J. Sun, S. T. Schneebeli, M. S. Nassar, C. A. Mirlin, J. F. Stoddart, *J. Am. Chem. Soc.* **2014**, *136*, 16651.

8 M. Yamaguchi, T. Ohba, T. Karatsu, S. Yagai, *Nat. Commun.* **2015**, *6*, 8936.

9 S. H. Jung, J. Jeon, H. Kim, J. Jaworski, J. H. Jung, *J. Am. Chem. Soc.* **2014**, *136*, 6446.

10 P. Cassagnau, *Polymer* **2008**, *49*, 2183.

11 P. Terech, D. Pasquier, V. Bordas, C. Rossat, *Langmuir* **2000**, *16*, 4485.

12 E. Daniel, A. G. Marangoni, *J. Am. Oil Chem. Soc.* **2012**, *89*, 749.

13 J. Yang, H. Yan, J. Dai, Z. Hu, H. S. Zhang, *J. Rheol. (Melville, NY, U. S.)* **2017**, *61*, 515.

14 A. B. Padmaperuma, L. S. Sapochak, P. E. Burrows, *Chem. Mater.* **2006**, *18*, 2389.

15 Y. Kawaguchi, Y. Itamura, K. Onimura, T. Oishi, *J. Appl. Polym. Sci.* **2005**, *96*, 1306.

16 Z.-C. Zhang, Z.-H. Sang, Y.-F. Huang, J.-F. Ru, G.-J. Zhong, X. Ji, R. Wang, Z.-M. Li, *ACS Sustainable Chem. Eng.* **2017**, *5*, 1692.

17 F. M. Menger, C. A. Littau, *J. Am. Chem. Soc.* **1993**, *115*, 10083.

18 Q. Huo, R. Leon, P. M. Petroff, G. D. Stucky, *Science* **1995**, *268*, 1324.

19 T. Wei, L. Lei, H. Kang, B. Qiao, Z. Wang, L. Zhang, P. Coates, K.-C. Hua, J. Kulig, *Adv. Eng. Mater.* **2012**, *14*, 112.

20 L. Kwisnek, J. Goetz, K. P. Meyers, S. R. Heinz, J. S. Wiggins, S. Nazarenko, *Macromolecules* **2014**, *47*, 3243.

21 M. Iizuka, R. Yamato, A. Fujimori, Control of hierarchical structure of crystalline nanofibers based on the cooperative phenomena of functional molecular group as the target of expression of new physical properties - creation of molecular conductors and enhancement of thixotropic ability -, in *Nanofiber Research: Researching New Highlight*, ed. by M. Rahman, InTech, **2016**, pp. 209–243. doi:10.5772/63701.

22 A. Fujimori, R. Yamato, T. Kikkawa, Y. Tatewaki, *J. Colloid Interface Sci.* **2015**, *448*, 180.

23 Q. Meng, S. Honda, Y. Tezuka, T. Yamamoto, A. Fujimori, *J. Polym. Sci., Part B: Polym. Phys.* **2016**, *54*, 486.

24 A. Fujimori, J. Kusaka, R. Nomura, *Polym. Eng. Sci.* **2011**, *51*, 1099.

25 P. H. Nam, N. Ninomiya, A. Fujimori, T. Masuko, *Polym. Eng. Sci.* **2006**, *46*, 39.

26 A. Fujimori, S. Arai, J. Kusaka, M. Kubota, K. Kurosaka, *J. Colloid Interface Sci.* **2013**, *392*, 256.

27 A. Fujimori, S. Arai, Y. Soutome, M. Hashimoto, *Colloids Surf., A* **2014**, *448*, 45.

28 H. Basit, A. Pal, S. Sen, S. Bhattacharya, *Chem.—Eur. J.* **2008**, *14*, 6534.

29 A. Fujimori, Y. Sugita, H. Nakahara, E. Ito, M. Hara, N. Matsuie, K. Kanai, Y. Ouchi, K. Seki, *Chem. Phys. Lett.* **2004**, *387*, 345.

30 A. Fujimori, T. Araki, H. Nakahara, E. Ito, M. Hara, H. Ishii, Y. Ouchi, K. Seki, *Chem. Phys. Lett.* **2001**, *349*, 6.

31 K. B. Blodgett, *J. Am. Chem. Soc.* **1935**, *57*, 1007.

© 2018 The Chemical Society of Japan

32 I. Langmuir, *J. Am. Chem. Soc.* **1917**, *39*, 1848.

33 A. Ulman, *An Introduction to Ultrathin Organic Films: From Langmuir-Blodgett to Self-Assembly*, Academic Press, Boston, **1991**. doi:10.1016/c2009-0-22306-3.

34 Q. Liu, Y. Wang, W. Li, L. Wu, *Langmuir* **2007**, *23*, 8217.

35 Y. Osada, J.-P. Gong, *Adv. Mater.* **1998**, *10*, 827.

36 K. Fukuda, T. Shiozawa, *Thin Solid Films* **1980**, *68*, 55.

37 V. Vand, I. P. Bell, *Acta Crystallogr.* **1951**, *4*, 465.

38 A. Maity, M. Gangopadhyay, A. Basu, S. Aute, S. S. Babu, A. Das, *J. Am. Chem. Soc.* **2016**, *138*, 11113.